

## Effects induced by hydroxyl radicals on salmon calcitonin: a RP-HPLC, CD and TEM study

Maria Cristina Gaudiano<sup>a</sup>, Marco Diociaiuti<sup>b,\*</sup>, Paola Bertocchi<sup>a</sup>, Luisa Valvo<sup>a</sup>

<sup>a</sup>*Dipartimento del Farmaco, Istituto Superiore di Sanità, Viale Regina Elena 299, 00161 Rome, Italy*

<sup>b</sup>*Dipartimento di Tecnologia e Salute, Istituto Superiore di Sanità, Viale Regina Elena 299, 00161 Rome, Italy*

Received 4 July 2002; received in revised form 23 July 2003; accepted 25 July 2003

### Abstract

The effects of hydroxyl radical attack on a peptidic drug were studied *in vitro*. Different chemico-physical techniques were used to investigate structural damage induced by oxidative stress conditions in salmon calcitonin (sCT), a peptide hormone used in treating osteoporosis. Reversed-phase liquid chromatography (RP-HPLC), circular dichroism (CD) and transmission electron microscopy (TEM) were applied to measure formation of oxidation/degradation products and to reveal the conformational and ultrastructural modifications in the presence of OH· free radicals. Hydroxyl radicals were obtained from ferrous sulfate and ascorbic acid mixtures. The RP-HPLC results revealed the formation of new chromatographic peaks indicating a number of degradation/oxidation products formed in the presence of OH· free radicals. CD spectra showed slight protein conformational modifications as well as aggregation. TEM confirmed sCT aggregation and suggested the formation of fibrillar aggregates.

© 2003 Published by Elsevier B.V.

**Keywords:** Oxidative stress; Hydroxyl radicals; Salmon calcitonin; RP-HPLC; CD; TEM

### 1. Introduction

Overproduction of hydroxyl radicals *in vivo* is a physiological condition during aging and in such pathologies as strokes, rheumatoid arthritis, cancer, Alzheimer's and Parkinson's diseases [1–5]. Under these conditions, the primary structure of endogenous and exogenous peptides and proteins could be modified leading to the formation of aggregates and fibrils [6]. This process has been described for the  $\beta$ -amyloid ( $\beta$ A) peptide, the central constituent of senile plaques in Alzheimer's disease. In this case, Met35 oxidation to sulfoxide enhances the aggregation rate compared to non-oxidized peptide [7]. In some cases, these peptide fibrils explicate cellular toxicity through an oxidative mechanism via a free radical pathway [8]. Schubert et al. [9] showed that aggregates of  $\beta$ A, amylin and human calcitonin from fibrillar deposits of medullary carcinomas were toxic to B12 cells. The authors proposed that the

toxicity was due to free radical-induced lipid peroxidation. Other authors reported that  $\beta$ A peptide is probably the source of free radical-mediated oxidative stress leading to neurodegeneration. The scientific literature increasingly indicates that free radicals can induce polypeptide aggregation by oxidative stress and it now seems evident that some peptide fibrils can induce oxidative reactions causing cell damage and toxicity [7,9]. However, the role of amyloid  $\beta$  protein aggregates as either mediators or by-products of pathogenic processes leading to Alzheimer's disease is still debated.

Bucciantini et al. [10] recently proposed that a common mechanism is involved in protein aggregate toxicity. They demonstrated that even aggregates of non-disease-associated proteins, very similar to amyloid fibrils and plaques, could be inherently highly toxic. The authors concluded that avoiding protein aggregation is crucial for the preservation of biological function and suggested common features in the origin of this family of protein deposition diseases.

In the present paper, the effect of OH· free radicals on salmon calcitonin (sCT) was studied *in vitro* to understand if radicalic oxidative reactions affect the degradation process of peptide in solution as well as its conformation and

\* Corresponding author. Tel.: +39-06-4990-2236; fax: +39-06-4938-7140.

E-mail address: [marco.diociaiuti@iss.it](mailto:marco.diociaiuti@iss.it) (M. Diociaiuti).

aggregation. sCT is a 32-amino acid polypeptide widely used in the treatment of such bone disorders as osteoporosis, hypercalcemia and Paget's disease. A Cys1–Cys7 disulfide bond and a Pro-amide residue at the C-terminus of the polypeptide chain [11,12] characterize the primary structure of sCT. In aqueous solution, the peptide is in a random coil conformation, but in the presence of organic solvents (i.e. trifluoroethanol, methanol) or phospholipids, sCT easily acquires an  $\alpha$ -helix secondary structure [13–15]. sCT has been shown to form amyloid fibrils *in vitro*. sCT aggregation was induced by vapor diffusion in the presence of DMPG and aggregates grown at 230 °C [16]. Both scanning and transmission electron microscopy (TEM) together with X-ray diffraction were used. The authors noted the formation of large aggregates and individual long fibers (up to 2000 nm) of 5–6 nm in diameter, very similar to those of A4/ $\beta$  peptide fragments from Alzheimer's disease. X-ray diffraction patterns for the large aggregates strongly suggested that sCT forms cross- $\beta$  fibrils. The overall structure of sCT is similar to that of human calcitonin (hCT), but they share only 16 of 32 residues [15]. Both peptides are therapeutically used. In spite of the similarity, hCT tends to aggregate in aqueous solutions faster than sCT, causing the formation of fibrillar precipitates [17,18]. hCT and sCT fibrillation studies based on turbidity measurements showed that both species aggregate over time. However, at the same concentration, sCT is much more stable [18]. Arvinte et al. [18] studied the structure of hCT fibrils by TEM, circular dichroism (CD) and Fourier transform infrared (FTIR) spectroscopy. They proposed a fibrillation model based on a double nucleation mechanism, previously described for gelation of sickle cell hemoglobin [19]. In this model, electrostatic interactions between hCT monomers are responsible for the initial aggregation step (homogeneous nucleation). Differences in the aggregation speed between hCT and sCT were attributed to the different  $pK$  values at pH 7.4 (8.7 and 10.4 for hCT and sCT, respectively). The resulting aggregate was spherical in shape.

In the second step, fibrils grew by fusion of spherical granules (heterogeneous nucleation). The quaternary structure evolution during fibrillation, leading to the largest supramolecular assembly, has been described in detail by Bauer et al. [17] in TEM experiments. Arvinte et al. [18] demonstrated that hCT molecules have, in the first aggregation step, both  $\alpha$ -helical and  $\beta$ -sheet secondary structure components. They proposed that “an intermolecular  $\beta$ -sheet component is formed by the tail residues 23–32. This  $\beta$ -sheet between hCT molecules, along with hydrophobic forces, provides a template for the  $\alpha$ -helical roads of residues 8–22 in the fibril formation”.

Aggregated and oxidized forms of hCT were observed *in vivo* in plasma under non-pathological conditions. Extracellular deposits of pro-calcitonin amyloid-like fibrils were found in medullary thyroid carcinomas [20]. As noted above, sCT shows a reduced propensity to the aggregation. This difference induces higher salmon peptide hypocalce-

mic potency, indicating that aggregation affects the pharmacological properties of the hormone [21].

The starting point of this work was the hypothesis that hydroxyl radicals are involved in the sCT peptide aggregation and fibrillar processes. The study was carried out *in vitro* to determine whether a direct cause–effect relationship could be hypothesized between hydroxyl attack on the peptide and its structural modifications, excluding the influence of metabolic modifications induced by the oxidative stress conditions *in vivo*. sCT was chosen for its lower propensity for aggregation compared to hCT, to exclude other possible peptide aggregation causes (i.e. hydrophobic and electrostatic interactions in the absence of oxidation reactions).

Reversed-phase liquid chromatography (RP-HPLC) was used to evaluate the effect of hydroxyl radicals on the degradation pathway of sCT in aqueous solution. The peptide conformational modifications induced by oxidative stress conditions were studied by CD. The ultrastructural rearrangements and the fibril formation were investigated by TEM. The study was carried out comparing the sCT samples in buffer and in the presence of mixtures of ferrous sulfate and ascorbic acid-producing  $OH\cdot$  free radicals *in vitro* [22].

## 2. Materials and methods

### 2.1. *In vitro* $OH\cdot$ free radicals production and quantification

$OH\cdot$  free radicals were produced by means of ferrous sulfate and ascorbic acid mixtures, as reported by Taglialatela et al. [22]. Stock solutions of ferrous sulfate (ACS reagent, Sigma, St. Louis, MO, USA) and L-ascorbic acid (minimum 99.0%, Sigma) were freshly prepared and mixed and diluted to obtain the oxidant mixtures ( $1 \times 10^{-4}$  M ferrous sulfate +  $2 \times 10^{-4}$  M ascorbic acid or  $0.5 \times 10^{-4}$  M ferrous sulfate +  $1 \times 10^{-4}$  M ascorbic acid).

These mixtures are highly sensitive to light, which accelerates  $OH\cdot$  free radical formation [23,24]. This phenomenon makes hydroxyl production non-reproducible because of the variable light exposition during the reaction. To address this problem and to ensure reproducible and rapid  $OH\cdot$  free radical formation, irradiation with a 60-W tungsten lamp was applied during the reaction. A 2-h oxidation time was set based on the results related to  $OH\cdot$  free radical production (see Section 3). LC control measurements were carried out on irradiated and non-irradiated oxidant mixtures to verify that no peaks were due to ascorbic acid or its degradation products.

Hydroxyl radical production from irradiated and non-irradiated oxidant mixtures was quantified by the coumarin method [25]. Coumarin-3-carboxylic acid (CCA) (99%, Aldrich-Chemical Co., Gillingham, UK) was added to oxidant mixtures to reach a final concentration of  $2 \times 10^{-4}$  M. CCA reacts with  $OH\cdot$  free radicals produced

by the mixture to yield the fluorescent compound 7-hydroxy-coumarin-3-carboxylic acid (7OHCCA). By excitation at 400 nm, 7OHCCA emits a fluorescence band centered at 450 nm. Fluorescence emission is proportional to 7OHCCA concentration and, consequently, to OH $\cdot$  free radical concentration. A calibration curve of 7OHCCA (99%, Aldrich-Chemical) standard solutions was employed to quantify hydroxyl radicals. Fluorescence spectra were recorded on FluoroMax spectrofluorimeter (Instrument S.A., Inc., JOBIN YVON/SPEX Division, Edison, NJ, USA). Fluorescence intensity was recorded at 450 nm; excitation was at 400 nm.

sCT CRS was obtained from European Pharmacopoeia (Strasbourg, France). All sCT samples were in 0.05 M sodium phosphate buffer, pH  $7.40 \pm 0.02$ . sCT solutions in the presence of oxidant mixtures were placed into a closed box 30 cm below a 60-W tungsten lamp. A 2-h oxidation time was applied. To allow comparison between sCT with and without the oxidant mixture, the same experimental procedure was performed on sCT solutions in buffer.

## 2.2. Reversed-phase liquid chromatography

LC analyses were conducted using a liquid chromatograph series 1100 (Agilent Technologies Deutschland GmbH, Waldbronn, Germany) equipped with an automatic injector (series G1329A, Agilent) and a diode array detector (series G1315B, Agilent).

sCT samples in phosphate buffer (0.5 mg/ml) as well as in the oxidant mixture (ferrous sulfate  $1 \times 10^{-4}$  M and ascorbic acid  $2 \times 10^{-4}$  M) were freshly prepared and analyzed after a 2-h reaction. To determine if hydroxyl radicals affect the degradation process of the peptide in solution, a slight modification of the European Pharmacopoeia LC method for the related peptides assay [26] was used to analyze the samples. A Hypersil ODS, 5  $\mu$ m,  $250 \times 4.0$  mm I.D. column (Alltech, Illinois, USA) was used. Eluent A was a mixture of 900 ml of buffer (3.26 g of tetramethylammonium hydroxide adjusted to pH 2.50 with phosphoric acid) and 100 ml of acetonitrile. Eluent B was a mixture of 400 ml of buffer (1.45 g of tetramethylammonium hydroxide adjusted to pH 2.50 with phosphoric acid) and 600 ml of acetonitrile. The mobile phase was delivered at a flow rate of 1.0 ml/min by linear gradient elution starting from A–B (72:28 v/v) to A–B (48:52 v/v) in 45 min. Column temperature was 40  $^{\circ}$ C. The chromatograms were recorded at 220 nm. Twenty microliters of the peptide solution was directly injected in buffer and in the oxidant mixture. Blank chromatograms were recorded as well as the chromatograms of sCT in buffer before and after light exposure to ensure that the light treatment itself did not affect the peptide degradation process.

Acetonitrile was HPLC-grade. All other chemicals were analytical grade.

## 2.3. Circular dichroism

CD spectra were recorded in the far-UV region (200–260 nm) using a Jasco J-710 spectropolarimeter (Jasco Corporation, Tokyo, Japan). All spectra were the average of four different scans and were blank subtracted. One-centimeter path-length quartz cell was employed. Measurements were performed at 0.2 nm spectral resolution on a 0.02 mg/ml peptide solution corresponding to  $1.9 \times 10^{-4}$  M in amino acid. Molar ellipticity was calculated based on the following formula:  $[\Theta] = \theta \times 100/l \times C$ , where  $\theta$  is the measured ellipticity in degrees,  $l$  is the cell path-length in centimeters and  $C$  is the sCT molar concentration calculated from the residues' mean molecular weight (107.2 Da). All CD measurements were carried out on freshly prepared peptide solutions.

## 2.4. Transmission electron microscopy

Negative staining of proteins is a rapid method that provides reliable structural information yet requires only a small amount of sample. The principle involves the embedding of electron-transparent specimen within a thin amorphous layer of heavy metal salt. Negative stain was obtained with a 2% w/v solution of phosphotungstate acid (PTA) buffered at pH=7.30 with NaOH. To avoid observation of salt precipitation from PTA or NaOH, which can be mistaken for biological structures, stain solution was filtered before each preparation on polycarbonate 0.2  $\mu$ m filters. Samples of 0.1 mg/ml sCT in 0.05 M phosphate buffer, pH  $7.40 \pm 0.02$ , and in the buffered oxidant mixture (ferrous sulfate  $1 \times 10^{-4}$  M and ascorbic acid  $2 \times 10^{-4}$  M) were analyzed by TEM as follows: a droplet of the solution was deposited onto 300 mesh copper grids for electron microscopy and covered with a very thin amorphous carbon film (about 20 nm). Excess liquid was removed by placing the grid on filter paper. When the grid was dry, a droplet of the stain solution was deposited and dried following the same procedure.

The samples were studied in a Zeiss 902 Transmission Electron Microscope operating at 80 kV. To enhance contrast, the microscope was settled with an Electron Energy Loss Imaging filter. This filter was settled to collect only elastic electrons ( $\Delta E=0$ ), to avoid the contribution of inelastic electrons to the contrast formation. Inelastic electrons scattered from the sample contribute only to image background noise and final image quality is strongly enhanced when they are filtered out [27]. The heavy metal (W) surrounding the particle scatters electrons more efficiently than the particle itself, providing enough image contrast and allowing detailed examination of the structure. Moreover, heavy metal salts provide good radiation protection and maintain specimen integrity. The resolution attained can be evaluated in the order of 2 nm [28].

### 3. Results and discussion

#### 3.1. Light effect on hydroxyl radicals production

In studies of the effect of oxidative stress on biological molecules *in vitro*, the production of free radicals is often a crucial point. In fact, OH· free radical production should be as similar as possible to that observed *in vivo*. Moreover, it must be reproducible, quantifiable and complete in a few hours.

In this work, OH· free radicals were produced by a mixture of ferrous sulfate and ascorbic acid [22]. This method, involving a redox reaction of iron ions, reproduces the OH· free radical formation mechanism observed in cells. Nevertheless, the reaction shows a low reproducibility *in vitro* because it is accelerated by light. To overcome this problem, reaction mixtures with and without calcitonin were irradiated with a 60-W tungsten lamp. A reproducible and complete production of OH· free radicals was observed after a 2-h irradiation. Longer irradiation times

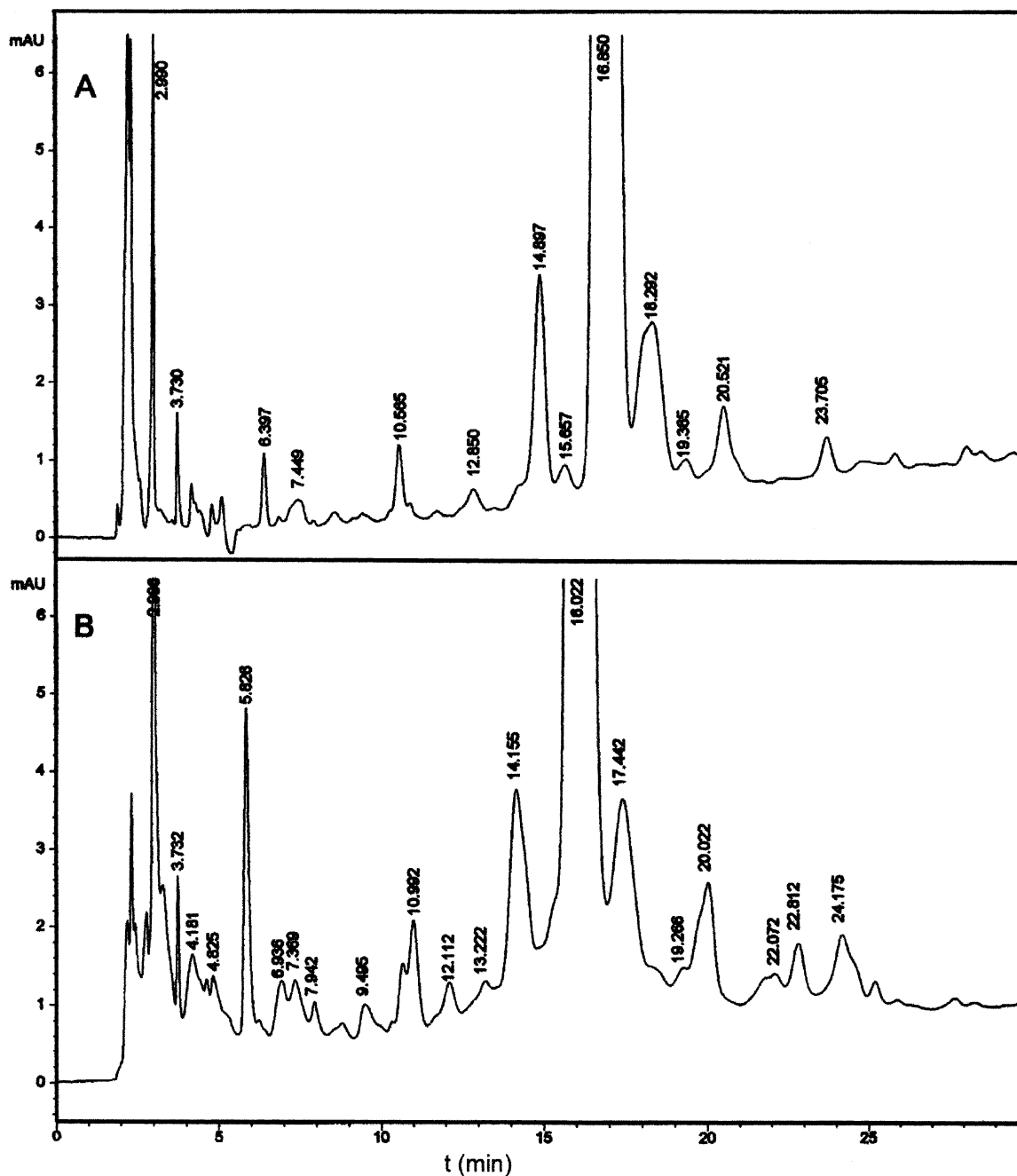


Fig. 1. RP-HPLC chromatograms of 0.5 mg/ml sCT in 0.05 M phosphate buffer solution, pH 7.40 (A) and in the presence of the oxidant mixture (ferrous sulfate  $1 \times 10^{-4}$  M and ascorbic acid  $2 \times 10^{-4}$  M in buffer) recorded after a 2-h reaction (B). Chromatographic conditions are reported in Section 2.1.



produced no increase of OH concentration, whereas shorter irradiation times caused lower hydroxyl radical production (data not shown). The hydroxyl radicals produced by the irradiated oxidant mixture consisting of ferrous sulfate  $1 \times 10^{-4}$  M and ascorbic acid  $2 \times 10^{-4}$  M were measured to be  $(0.81 \pm 0.05) \times 10^{-5}$  M, while those produced by the half concentrated irradiated oxidant mixture were  $(0.57 \pm 0.01) \times 10^{-5}$  M. The same non-irradiated solutions produce  $(0.37 \pm 0.02) \times 10^{-5}$  and  $(0.35 \pm 0.01) \times 10^{-5}$  M of hydroxyl radicals, respectively.

### 3.2. RP-HPLC analysis

Fig. 1A and B report the chromatographic profiles of sCT in buffer and after the oxidant treatment. Fig. 1A shows the presence of a principal peak at 16.85 min, corresponding to the retention time of the hormone, and many small peaks at higher and lower retention time due to impurities and degradation products of the peptide. In fact, sCT in aqueous solutions is known to undergo hydrolysis resulting in cleavage of 1–2 amide bond, deamination of the Gln<sup>14</sup> and Gln<sup>20</sup> residues, sulfide exchange and dimerization [29]. The HPLC analysis of the same sample after a 2-h irradiation gave the same chromatographic profile, indicating that the drug structure was not affected by light exposure when ferrous sulfate and ascorbic acid were not added (data not shown).

Fig. 1B shows a different chromatographic profile of the peptide in solution after reaction with hydroxyl radicals. In particular, a new peak can be observed at 5.83 min and other small peaks before and after the sCT peak. An area increase of the peak at about 14 min and of other peaks at a higher retention time than that for sCT can also be observed. Both chromatographic profiles are complex but indicate that the degradation pathway of sCT in the presence of hydroxyl radicals is different from that of the hormone in buffer both because new products form and because existing products increase. This result indicates that the reaction with OH· radicals affects the stability of the peptide primary structure, increasing the number of degradation products. Further studies are underway to examine how the peptide is modified by the OH· free radicals. In the absence of the drug, irradiated oxidant mixtures showed no peaks in the 3–30 min time range, demonstrating that none of the peaks detected in the chromatogram of sCT after the oxidant treatment were from ascorbic acid or its degradation products (data not shown).

### 3.3. CD data

To evaluate the effect of OH· free radicals on the conformation of sCT, CD spectra were recorded on peptide solutions in buffer and in the oxidant mixtures. Fig. 2 shows CD spectra in the peptide-bond absorption region (200–260 nm) of irradiated sCT in phosphate buffer (curve a) and in oxidant mixtures (curves b and c). This spectral region is

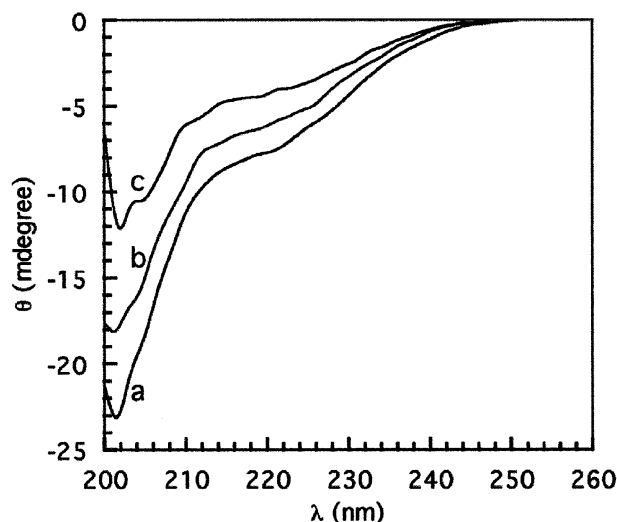


Fig. 2. Circular dichroism spectra of 0.02 mg/ml sCT in 0.05 M phosphate buffer (curve a), in the presence of ferrous sulfate  $0.5 \times 10^{-4}$  M and ascorbic acid  $1 \times 10^{-4}$  M (curve b) and in the presence of ferrous sulfate  $1 \times 10^{-4}$  M and ascorbic acid  $2 \times 10^{-4}$  M (curve c), recorded after a 2-h reaction.

sensitive to peptide conformation and both the shape and intensity of dichroic band depend on peptide secondary structure. As previously reported in literature [11,15], sCT assumes a random-coil conformation in water solution at pH 7.4. A typical negative band characterizes the CD spectrum with a minimum at about 200 nm [30]. The superposition of CD spectra obtained from irradiated and non-irradiated sCT in buffer, without the oxidant mixture, indicates that the simple lamp irradiation procedure did not affect peptide conformation (data not shown). Moreover, the molar ellipticity of sCT in buffered aqueous solution is in good agreement with published data [11,15].  $[\theta]$ , calculated using the formula reported in Section 2.3, is about  $12\,300 \text{ degree cm}^2 \text{ dmol}^{-1}$ . A clear decrease in intensity was observed in the presence of oxidant mixtures. This behavior could be attributed to the peptide aggregation phenomena. Fibrillation leads to a phase separation and the largest fibrils tend to precipitate, leading to a lower effective peptide concentration in the CD experiment. However, initial nucleation cores and small protofibrils can always participate in the dichroic scattering. In fact, peptide aggregation is also associated with slight conformational variations, as suggested by the appearance in the CD spectra of a new shoulder, located at about 205 nm. This shoulder appeared in the curve for the less oxidized preparation (b) and is quite evident in the curve for the more oxidized one (c). Moreover, this contribution modifies the shape of the entire curve c, even at higher  $\lambda$  values. Arvinte et al. [18] described the mechanism of hCT fibrillation. Especially in the first fibrillation stage, when the coexistence of fibrillar structures and granules was observed, they showed that the CD spectrum changed from a single minimum spectrum (at about 200 nm), characteristic of the random coil conforma-

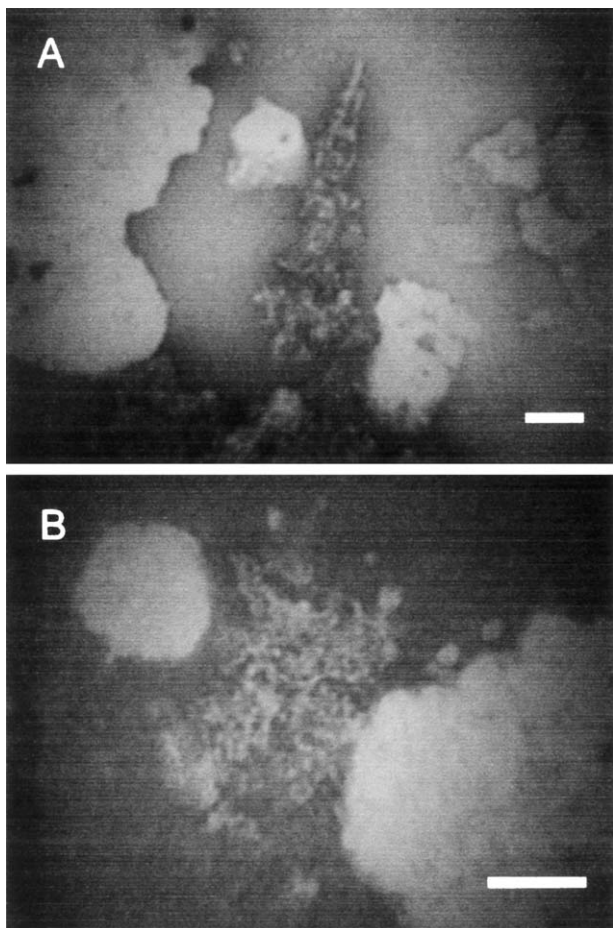


Fig. 3. Transmission electron microscopy images of 0.1 mg/ml sCT in 0.05 M phosphate buffer solution, after a 2-h reaction. Bars represent 100 nm in both A and B.

tion, to a double minima spectrum (at about 205 and 215 nm), related to a 17%  $\alpha$ -helical content (mature fibers showed up to 25% content). Moreover, FTIR results demonstrated that  $\beta$ -sheet components were also present. The authors concluded that a two-step mechanism was responsible for the fibrillation process.

The CD data obtained in our experiments could be interpreted in the light of published CD spectra [18]. The main differences in the two experiments were the different species used (hCT and sCT) and the way in which aggregation was induced. In fact, sCT is more stable than hCT [18] and our method induced a more gradual oxidation. Consequently, we think we have observed for sCT the early stage of the fibrillation process proposed for hCT.  $\alpha$  and  $\beta$  components, responsible for the modification of the CD spectrum in the experiment of Arvinte et al. after about a 30-min warming at 40 °C, were likely responsible for the same modification observed in our experiment in curve c, related to the more oxidized preparation. In fact, the two spectra are very similar.

CD data indicate that the reaction with hydroxyl radicals can affect the secondary structure of the peptide as well as its aggregation state because of the modifications occurring in the primary sequence, as demonstrated by RP-HPLC results. The effect observed by CD is higher in the more concentrated oxidant mixture (curve c), indicating that the conformational variations and aggregations depend on hydroxyl radical concentration.

### 3.4. TEM data

TEM measurements were carried out to verify the hypothesis that sCT aggregates in the presence of  $\text{OH}\cdot$  free radicals.

Fig. 3 shows micrographs relative to sCT in non-oxidized buffer solution. Both images show clusters of round units of about 7 nm in diameter. Circular units are grouped in a cluster, probably because of the sample preparation, during which a solution droplet was dried onto amorphous carbon. However, the single units are well separated from each

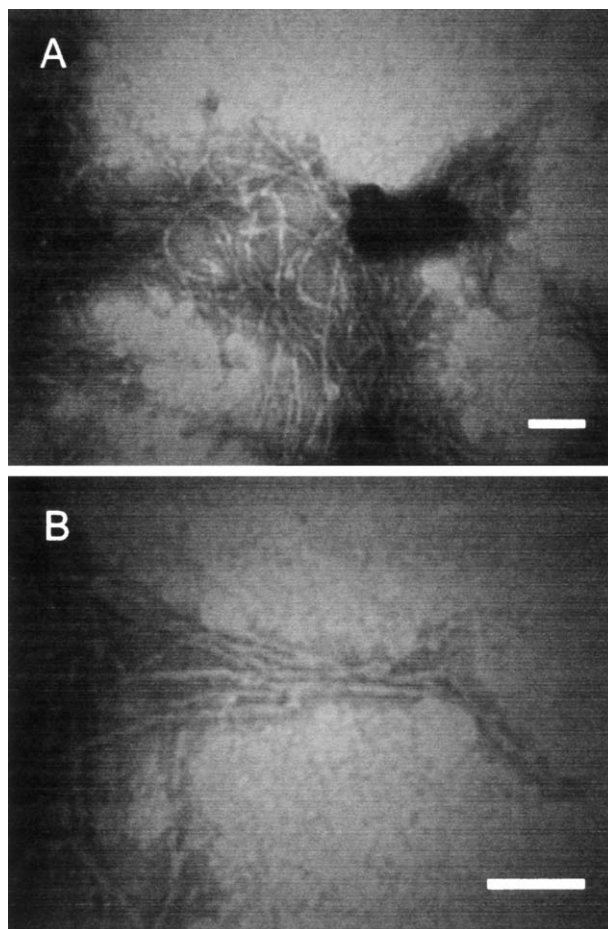


Fig. 4. Transmission electron microscopy images of 0.1 mg/ml sCT in the presence of the oxidant mixture (ferrous sulfate  $1 \times 10^{-4}$  M and ascorbic acid  $2 \times 10^{-4}$  M), after a 2-h reaction. Bars represent 100 nm in both A and B.

other, even if a tendency to a fiber-like aggregation can be observed in image A. This could be an early stage of the sCT aggregation process that spontaneously occurs at a low rate even in buffer solution. The presence of granular and punctuate aggregates has also been reported, during the first fibrillation step, in the paper of Arvinte et al. [18].

Fig. 4, for sCT in the presence of oxidant mixture, is dramatically different from Fig. 3. Images clearly show defined fibers of about 7–8 nm in diameter, organized in large skeins or in ribbons. These images are very similar to those published for hCT by Bauer et al. [17] and Arvinte et al. [18]. Gilchrist and Bradshaw [16] observed similar fibrils, for sCT aggregation induced within 9 days by heating the samples at 230 °C in the presence of DMPG. The authors demonstrated a strong similarity between amyloid fibrils of sCT and  $\beta$ A and proposed the cross- $\beta$  structure for both proteins.

TEM images did not reveal differences between sCT in buffer before and after light exposure, in the absence of oxidant mixture, indicating that the drug conformation was not affected by light treatment when ferrous sulfate and ascorbic acid were not added (data not shown).

#### 4. Conclusions

The results obtained demonstrate that OH $\cdot$  free radicals strongly affect the structure of sCT. As shown by RP-HPLC, hydroxyl radicals induced new degradation products. CD spectra revealed a sharp decrease in the intensities because of the aggregation process leading to phase separation in the solution. sCT molecules remaining in solution showed small changes in the secondary structure, probably due to the early stage of the aggregation process. TEM results gave information on the structure of the aggregates. The fibers observed were very similar to those obtained by the heating procedure, suggesting that the mechanism of fiber formation is independent from the producing agent. These fibrils are amyloid, similar to those already observed in vivo for hCT in carcinoma medullary plaques.

In general, we think that it is important to avoid the sCT aggregation process because it is associated with therapeutic inefficacy of the hormone drug. Moreover, there is a general tendency to consider amyloid-like fibrils and protofibrils to be toxic. Our results, showing a correlation between oxidative stress and fibrillar process for sCT, raise questions about the efficacy and safety of the use of this drug in physiopathological conditions characterized by overproduction of hydroxyl radicals.

#### Acknowledgements

This research is supported by a grant of the National Health Fund for the project “Safety of Drugs Used in Diseases of the Elderly”.

The authors thank Prof. L. Annunziato of the University “Federico II” of Naples and Dr. O. Sapora of Istituto Superiore di Sanità of Rome for their advice. The authors are also grateful to Dr. F. Ciaffoni and to Mr. C. De Sena for their technical assistance.

#### References

- [1] R.G. Cutler, L. Packer, J. Bertram, A. Mori, *Oxidative Stress and Aging*, Birkhauser Verlag, Basel, 1995.
- [2] P. Jenner, Oxidative damage in neurodegenerative disease, *Lancet* 344 (1994) 796–798.
- [3] E.Y. Yang, S.X. Guo-Ross, S.C. Bondy, The stabilization of ferrous iron by a toxic beta-amyloid fragment and by an aluminum salt, *Brain Res.* 839 (1999) 221–226.
- [4] S. Toyokuni, Iron-induced carcinogenesis: the role of redox regulation, *Free Radic. Biol. Med.* 20 (1996) 553–566.
- [5] B. Halliwell, J.M.C. Gutteridge, Role of free radicals and catalytic metal ions in human disease: an overview, *Methods Enzymol.* 186 (1990) 1–85.
- [6] R.P. Mason, D.N.R. Rao, Thiyl free radical metabolites of thiol drugs, glutathione, and proteins, *Methods Enzymol.* 186 (1990) 318–329.
- [7] S.W. Snyder, U.S. Lador, W.S. Wade, G.T. Wang, L.W. Barrett, E.D. Matayoshi, H.J. Huffaker, G.A. Krafft, T.F. Holzman, Amyloid-beta aggregation: selective inhibition of aggregation in mixtures of amyloid with different chain lengths, *Biophys. J.* 67 (1994) 1216–1228.
- [8] C.J. Kay, Mechanochemical mechanism for peptidyl free radical generation by amyloid fibrils, *FEBS Lett.* 403 (1997) 230–235.
- [9] D. Schubert, C. Behl, R. Lesley, A. Brack, R. Dargusch, Y. Sagara, H. Kimura, Amyloid peptides are toxic via a common oxidative mechanism, *Proc. Natl. Acad. Sci. U. S. A.* 92 (1995) 1989–1993.
- [10] M. Bucciattini, E. Giannoni, F. Chiti, F. Baroni, L. Formigli, J. Zurdo, N. Taddei, G. Ramponi, C.M. Dobson, M. Stefani, Inherent toxicity of aggregates implies a common mechanism for protein misfolding diseases, *Nature* 416 (2002) 507–511.
- [11] G. Siligardi, B. Samori, S. Melandri, M. Visconti, A.F. Drake, Correlations between biological activities and conformational properties for human, salmon, eel, porcine calcitonins and Elcatonin elucidated by CD spectroscopy, *Eur. J. Biochem.* 221 (1994) 1117–1125.
- [12] A. Motta, M.A. Morelli, N. Goud, P.A. Temussi, Sequential  $^1\text{H}$  NMR assignment and secondary structure determination of salmon calcitonin in solution, *Biochemistry* 28 (1989) 7996–8002.
- [13] J.P. Meyer, J.T. Pelton, J. Hoflack, V. Saudek, Solution structure of salmon calcitonin, *Biopolymers* 31 (1991) 233–241.
- [14] R.M. Epand, R.F. Epand, R.C. Orlowski, R.J. Schlueter, L.T. Boni, S.W. Hui, Amphipathic helix and its relationship to the interaction of calcitonin with phospholipids, *Biochemistry* 22 (1983) 5074–5084.
- [15] T. Arvinte, A.F. Drake, The structure and mechanism of formation of human calcitonin fibrils, *J. Biol. Chem.* 268 (1993) 6408–6414.
- [16] P.J. Gilchrist, J.P. Bradshaw, Amyloid formation by salmon calcitonin, *Biochim. Biophys. Acta* 1182 (1993) 111–114.
- [17] H.H. Bauer, U. Aebi, M. Haner, R. Hermann, M. Muller, T. Arvinte, H.P. Merkle, Architecture and polymorphism of fibrillar supramolecular assemblies produced by in vitro aggregation of human calcitonin, *J. Struct. Biol.* 115 (1995) 1–15.
- [18] T. Arvinte, A. Cudd, A.F. Drake, The structure and mechanism of formation of human calcitonin fibrils, *J. Biol. Chem.* 268 (1993) 6415–6422.
- [19] F.A. Ferrone, J. Hofrichter, H.R. Sunshine, W.A. Eaton, Kinetic studies on photolysis-induced gelation of sickle cell hemoglobin suggest a new mechanism, *Biophys. J.* 32 (1980) 361–380.
- [20] P.H. Tobler, F.A. Tschopp, M.A. Dambacher, W. Born, J.A. Fischer, Identification and characterization of calcitonin forms in plasma and

- urine of normal subjects and medullary carcinoma patients, *J. Clin. Endocrinol. Metab.* 57 (1983) 749–754.
- [21] D.F. Moriarty, S. Vagts, D.P. Raleigh, A role for the C-terminus of calcitonin in aggregation and gel formation: a comparative study of C-terminal fragments of human and salmon calcitonin, *Biochem. Biophys. Res. Commun.* 245 (1998) 344–348.
- [22] M. Taglialatela, P. Castaldo, S. Iossa, A. Pannaccione, A. Fresi, E. Ficker, L. Annunziato, Regulation of the human ether-a-gogo related gene (HERG) K<sup>+</sup> channels by reactive oxygen species, *Proc. Natl. Acad. Sci. U. S. A.* 94 (1997) 11698–11703.
- [23] J. Van der Zee, B.B. Krootjes, C.F. Chignell, T.M. Dubbelman, J. Van Steveninck, Hydroxyl radical generation by a light-dependent Fenton reaction, *Free Radic. Biol. Med.* 14 (1993) 105–113.
- [24] M.K. Shih, M.L. Hu, UVA-potentiated damage to calf thymus DNA by Fenton reaction system and protection by *para*-aminobenzoic acid, *Photochem. Photobiol.* 63 (1996) 286–291.
- [25] S.W. Botchway, S. Chakrabarti, G.M. Makrigiorgos, Novel visible and ultraviolet light photogeneration of hydroxyl radicals by 2-methyl-4-nitro-quinoline-*N*-oxide (MNO) and 4,4'-dinitro-(2,2')bipyridinyl-*N,N'*-dioxide (DBD), *Photochem. Photobiol.* 67 (1998) 635–640.
- [26] Council of Europe, European Pharmacopoeia, 3rd ed., EDQM, Strasbourg, 1997, p. 1487.
- [27] R.F. Egerton, *Electron Energy Loss Spectroscopy*, Plenum, New York, 1986.
- [28] R.C. Valentine, B.M. Shapiro, E.R. Stadtman, Regulation of glutamine synthetase: XII. Electron microscopy of the enzyme from *Escherichia coli*, *Biochemistry* 7 (1968) 2143–2152.
- [29] V. Windisch, F. DeLuccia, L. Duhau, F. Herman, J.J. Mancel, S.-Y. Tang, M. Vuilhorgne, Degradation pathways of salmon calcitonin in aqueous solution, *J. Pharm. Sci.* 86 (1997) 359–364.
- [30] R.W. Woody, A. Koslowski, Recent developments in the electronic spectroscopy of amides and  $\alpha$ -helical polypeptides, *Biophys. Chem.* 101–102 (1) (2002) 535–551.